Available online at www.sciencedirect.com
ScienceDirect
Earth and Planetary Science Letters 269 (2008) 1 – 10
EPSL
www.elsevier.com/locate/epsl

A Late Miocene acceleration of exhumation in the Himalayan crystalline core

Cameron Wobus [a,*], Malcolm Pringle [b], Kelin Whipple [c], Kip Hodges [c]

[a] CIRES, Campus Box 216, University of Colorado, Boulder, CO 80309, United States
[b] Department of Earth and Planetary Sciences, Massachusetts Institute of Technology, Cambridge, MA 02139, United States
[c] School of Earth and Space Exploration, Arizona State University, Tempe, AZ 85287-1404, United States

Received 10 July 2007; received in revised form 7 January 2008; accepted 11 February 2008
Available online 4 March 2008
Editor: C.P. Jaupart

Abstract

Unraveling the relative roles of erosion and tectonics in shaping the modern topography of active orogens requires datasets documenting spatial and temporal patterns of exhumation, surface uplift and climatic forcing throughout orogenic growth. Here we report the results of biotite $^{40}Ar/^{39}Ar$ incremental heating and single-grain laser-fusion experiments from a nearly vertical, ~1000 m age-elevation transect in the central Nepalese Himalaya. Age-elevation relationships constructed from these data suggest very slow cooling in this part of the Himalayan crystalline core during the Early Miocene, accelerating to only moderate rates at ~10 Ma. If we assume purely vertical exhumation and a steady-state thermal structure, the exhumation rates implied by these data are ≪0.1 mm/yr prior to 10 Ma and ~0.5 mm/yr from ~10–7 Ma. The acceleration in cooling rate at 10 Ma requires a change in kinematics that may be linked to large-scale changes in climate, or to more local tectonic perturbations. Although we do not presently have enough data to assess the relative roles of regional vs. local drivers, these data provide a new constraint on exhumation through the Miocene that must be honored by any model of Himalayan evolution.

Keywords: Himalaya; argon thermochronology; tectonics; climate

1. Introduction

The central Nepalese Himalaya reflects extremes in both tectonics and erosion: a series of thrust faults at the base of the range accommodates approximately 20 mm/yr of convergence between India and Eurasia, while the South Asian monsoon drops over 3 m of rain along the rangefront in a typical season (e.g., Bookhagen and Burbank, 2006). Because the tectonic and climatic signals are both strong in this region, the Himalaya has become a centerpiece in the debate surrounding the degree to which climate and tectonics may be coupled at the orogen scale (e.g., Burbank et al., 2003; Thiede et al., 2004; Wobus et al., 2005; Huntington et al., 2006). Most of these studies cite thermochronologic datasets in which spatial or temporal changes in cooling ages are used as proxies for spatial or temporal changes in exhumation over Pliocene–Recent timescales. However, the strongest climatic signal to have affected the Himalaya is likely to have occurred much earlier (>20 Ma) when recent evidence suggests that South and East Asian monsoon climates were established (Sun and Wang, 2005; Clift, 2006). In addition, a variety of evidence suggests there were substantial shifts in both climate and tectonics in the region in the Late Miocene (~8–10 Ma) (e.g., Kroon et al., 1991; Molnar et al., 1993; Garzione et al., 2000). Pinpointing the timing of such regional "events" – and understanding the degree to which large climatic changes influence local and regional tectonics – requires an orogen-wide database documenting changes in exhumation rates through this period.

Toward this end, we report here the results from a new $^{40}Ar/^{39}Ar$ age-elevation transect in the Langtang valley of central Nepal, documenting cooling of the Greater Himalayan Sequence through the ~350 °C isotherm. Our data include

* Corresponding author.
E-mail address: cameron.wobus@colorado.edu (C. Wobus).

0012-821X/$ - see front matter © 2008 Elsevier B.V. All rights reserved.
doi:10.1016/j.epsl.2008.02.019

single-grain laser-fusion and bulk incremental heating analyses of biotites from the Greater Himalayan sequence, which represents the metamorphic core of the Himalaya. This new dataset is one of the few available that allows direct estimates of cooling rates and patterns in central Nepal through the Miocene (e.g., Vannay and Hodges, 1996; Huntington et al., 2006). As a result, our data provide much-needed constraints on the tectonic evolution of the Himalaya that must be honored by any conceptual or numerical model of early Himalayan orogenesis.

2. Background

Convergence between India and Eurasia – currently estimated at approximately 20 mm/yr based on geodetic observations (Bilham et al., 1997) – is accommodated along the Main Himalayan Thrust (MHT), which represents the main décollement separating the two plates. While the exact subsurface geometry and the timing of activity on surface thrusts remain the topics of active research (e.g., Lave and Avouac, 2001; Wobus et al., 2005; Bollinger et al., 2006), there is general agreement that the MHT splays into three major surface thrust systems to the south of the High Himalaya (Fig. 1) (Hodges, 2000). Of these, the northernmost structure – referred to as the Main Central Thrust system (MCT) – represents the most prominent metamorphic transition, separating primarily greenschist facies rocks in the footwall from amphibolite and higher grade rocks in the hanging wall. Where the MCT is well mapped, it is characterized by a broad (~1 km) shear zone, with evidence for Pliocene to Quaternary brittle deformation in many locations, including in the Langtang valley (Macfarlane et al., 1992; Hodges, 2000; Hodges et al., 2004). In tectonic models that invoke a coupling between focused erosion and extrusion of a low-viscosity "crustal channel", the rocks in the hanging wall of the MCT – referred to as the Greater Himalayan Sequence (GHS) – represent the exhumed remnants of this extruded channel (Beaumont et al., 2001; Grujic et al., 2002). An alternative model of Himalayan tectonics that calls upon tectonic underplating and duplex formation to grow the high range has also been proposed (e.g., Robinson et al., 2003; Pearson and DeCelles, 2005; Bollinger et al., 2006). Due in large part to the lack of complete cooling histories for rocks from the GHS and the underlying Lesser Himalayan Sequence, either of these models can be shown to be consistent with available data (Wobus et al., 2006) — although the latter model requires a more restrictive set of parameters. Building a more complete exhumation history of the GHS is therefore an important prerequisite for understanding how the central Nepalese Himalaya evolved between the Early Miocene and the present.

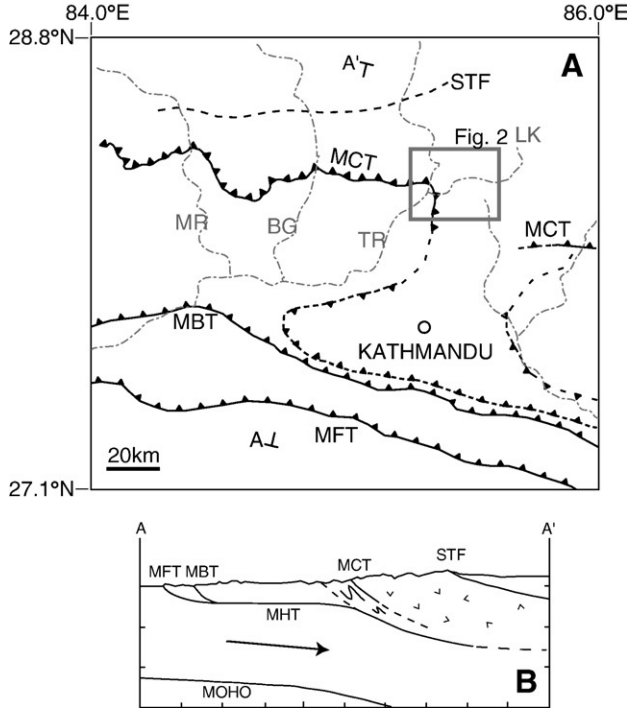

Fig. 1. Regional tectonic setting. A) Location of major thrust systems in central Nepalese Himalaya. MFT = Main Frontal Thrust; MBT = Main Boundary Thrust; STF = South Tibetan Fault system. Grey dash-dot lines are major rivers for reference: LK = Langtang Khola; TR = Trisuli River; BG = Burhi Gandaki River; MR = Marsyandi River. B) Schematic cross-section through central Nepalese Himalaya, showing relationship of surface thrusts to Main Himalayan Thrust (MHT). Patterned region between MCT and STF is Greater Himalayan Sequence (GHS). Figure adapted from Wobus et al. (2005).

Available geochronologic data from the GHS in Nepal and India typically indicate cooling of this metamorphic core through ~350 °C in the Early–Middle Miocene (e.g., Hubbard and Harrison, 1989; Copeland et al., 1991; Macfarlane, 1993; Vannay et al., 2004). In general, these inferences are based on results from individual bedrock samples, and therefore do not yield insights into the temporal patterns of exhumation in the GHS through this interval. One pattern that consistently emerges from previous geochronology on the GHS, however, is a general younging of cooling ages structurally down-section within ~5–10 km of the MCT (Hubbard and Harrison, 1989; Copeland et al., 1991; Macfarlane, 1992). $^{40}Ar/^{39}Ar$ cooling ages as young as the Late Pliocene (~2–3 Ma) have been documented from within the MCT zone in the nearby Marsyandi valley (Edwards, 1995), and in the Langtang valley (Macfarlane, 1993). Young $^{40}Ar/^{39}Ar$ cooling ages such as these are generally interpreted as reflecting either out-of-sequence brittle motion within the MCT zone (Macfarlane, 1993; Hodges et al., 2004), or late-stage hydrothermal activity within the MCT zone (Copeland et al., 1991) in the Pliocene.

Previous estimates of exhumation rates in the Himalaya are most commonly based on valley-bottom samples and/or low-temperature thermochronometers. As a result, these datasets typically require some assumptions about the thermal structure of the upper crust, and provide information on exhumation rates only since the Pliocene. Estimated Pliocene–Recent exhumation rates commonly exceed 2 mm/yr based on low-temperature thermochronology (Sorkhabi et al., 1996; Burbank et al., 2003; Thiede et al., 2004). An age-elevation transect in the nearby Marsyandi valley suggests considerably slower rates (~0.5 mm/yr) in the Early Pliocene (Huntington et al., 2006), consistent with the average rates that can be inferred from $^{40}Ar/^{39}Ar$ ages of 15–20 Ma commonly reported from higher in the GHS section throughout the Himalayan arc (e.g., Hubbard

and Harrison, 1989; Macfarlane, 1993; Vannay and Hodges, 1996; Vannay et al., 2004; Viskupic et al., 2005). Combined, these varied datasets suggest that exhumation rates in the Himalaya accelerated sometime after the Early Miocene. However, few studies have been able to document when such an acceleration may have occurred (e.g., Huntington et al., 2006).

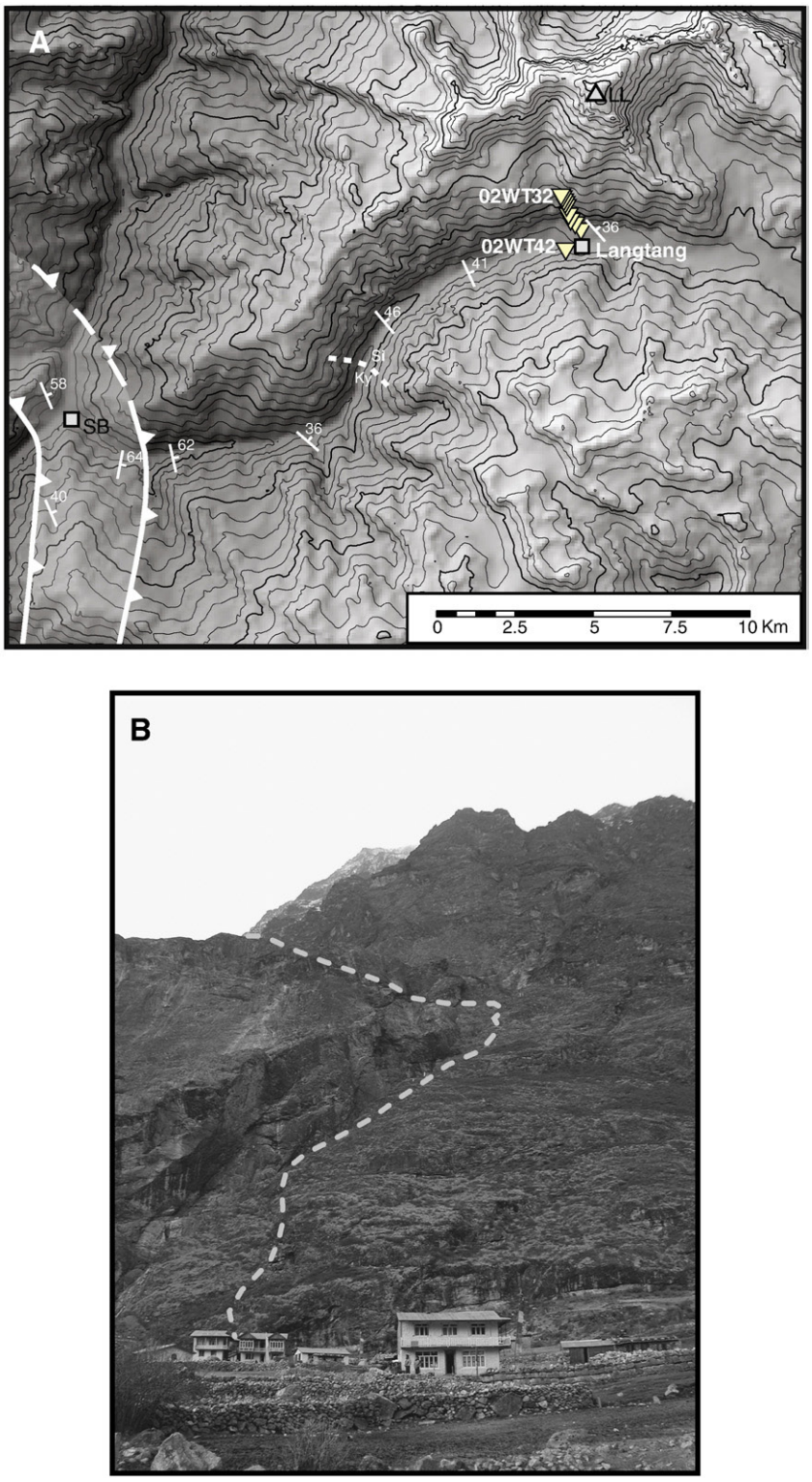

Fig. 2. A) Study area location map. Barbed lines represent approximate upper and lower bounds of Main Central Thrust zone, as mapped by Macfarlane et al. (1992). Dashed line approximately halfway up valley delineates Sillimanite-in isograd, as mapped by Reddy et al. (1993) (Ky = Kyanite; Sil = Sillimanite). Triangles immediately north of the village of Langtang show sample locations. SB = Syabrubensi. LL = Langtang Lirung. Subset of structural measurements are shown by standard strike-dip symbols with dips adjacent to symbols. B) View to the north of the valley wall from which samples were taken. Approximate path of lower 2/3 of age-elevation transect is shown by dashed grey line. Village of Langtang is in foreground.

In order to document temporal patterns of exhumation within the core of the GHS, we focused our study on the Langtang valley of central Nepal, a deep glacial valley approximately 60 km north of the capital city of Kathmandu. Our sampling transect is along the northern wall of this glacial valley near the town of Langtang, approximately 15 km to the northeast of the northern limits of the MCT zone (Macfarlane et al., 1992) (Fig. 2). Bedrock exposure throughout the Langtang valley is exceptional, which has allowed the GHS to be divided into four lithologic units here (Inger and Harris, 1993; Reddy et al., 1993); all of these units correlate to the Formation I pelitic gneiss of Le Fort (Le Fort, 1975).

In most of the lower Langtang valley, the GHS consists of metapelitic rocks of the Syabru Unit, which is kyanite grade in the immediate hanging wall of the MCT zone and grades upsection to sillimanite grade approximately halfway between the villages of Syabrubensi and Langtang (Fig. 2). In the uppermost Syabru Unit, locally developed migmatite and leucogranitic dikes become common. The Kyangjin Unit, which structurally overlies the Syabru Unit, consists of a biotite-rich augen gneiss with feldspar augen ~2–3 cm in diameter. Reddy et al. (1993) suggested that the contact between the Syabru and Kyangjin Units may be tectonic in origin, but they interpreted this structure as pre-Early Miocene, thus pre-dating deformation in the MCT zone (e.g., pre-Early Miocene). The two units structurally overlying the Kyangjin Unit – referred to as the Langshisa Unit and Langtang Lirung Unit – comprise psammitic metasedimentary rocks with increasing proportions of leucogranitic intrusions upsection.

3. Methods

We collected our samples from fresh outcrops along a nearly vertical, ~1000 m transect on the northern wall of the Langtang valley (Fig. 2). Elevations along the transect were recorded using a hand-held altimeter. Repeat elevation measurements collected at the base of the transect before and after our samples were collected suggest an uncertainty in our sample elevations of ±15 m. All of the outcrops comprise high-grade metamorphic rocks with mineral assemblages consistent with pelitic protoliths. Lithologies are dominated by schists and migmatites, with three samples of a K–feldspar–quartz–biotite augen gneiss near the top of the transect. Based on comparisons of our field descriptions and rock samples with the lithologic divisions proposed by Reddy et al. (1993), we assign the lowermost six samples in our transect to the Syabru Unit, and the uppermost four samples to the Kyangjin Unit. Substantial lithologic heterogeneity within these metamorphic assemblages makes these assignments tentative, however. Foliations throughout the transect dip to the northeast at 30–40°, with shear sense indicators, where present, indicating top-to-the-southwest sense of shear. Although muscovite is locally present, micas are dominated by biotite throughout the section.

Due to the prevalence of biotite as the potassium-bearing phase, we focused our thermochronology on the biotite $^{40}Ar/^{39}Ar$ thermochronometer, which has a nominal closure temperature of ~350 °C (Hodges, 2003). Samples were crushed, washed, and sieved and biotites were separated by standard mineral separation techniques. Final selection of biotites for analysis was conducted by hand under a binocular microscope to ensure sample purity. Samples were then irradiated without Cadmium shielding at the McMaster University nuclear reactor in Hamilton, Ontario, using Taylor Creek sanidine as the neutron flux monitor.

$^{40}Ar/^{39}Ar$ ages for each sample were measured in two ways. First, we loaded ten single-grain aliquots of each sample in to 2 mm wells in Cu planchets for analysis by laser fusion. Filled planchets were loaded into the vacuum system and baked out at 320–350 °C for 8 h to minimize contamination of the cooling signal from loosely held argon. Following this bakeout, gas was liberated by total fusion of each single-grain using an 810 nm diode laser, ramping from 0 to 15 W over 30 s to minimize jumping of the bioite grains and then held at 15 W for 15 s to ensure complete fusion. The released gas was cleaned up for 10 min using a SAES glass AP10GP getter operated at ~650 °C and a SAES C50 St101 getter operated at 350 °C, followed by analysis with a single electron multiplier detector on a MAP 215-50 mass spectrometer using peak hopping over 10 complete peak cycles.

Our second set of analyses was conducted using incremental heating experiments on multi-grain samples. Aliquots of irradiated biotite grains ranging from 2.3 to 39.5 mg were loaded into copper foil packets and placed under vacuum. Gas was liberated from these samples with an 18-step-heating schedule between ~700 and 1400 °C on a double vacuum low blank resistance furnace using a Tantalum main crucible with a Molybdenum inner liner. Individual heating steps were 15 min long; gas cleanup continued while the crucible cooled for an additional 10 min of exposure to two SAES C50 St101 getters operated at room temperature and 350 °C, plus a stainless steel finger filled with 1 g of degassed 10A synthetic molecular sieve. The remaining gas was similarly analyzed with a single electron multiplier detector on a MAP 215-50 mass spectrometer using peak hopping over 10 cycles.

Data reduction for all samples was performed using ArArCalc Version 2.2 (Koppers, 2002). All ages are reported relative to Taylor Creek sanidine at 28.34 Ma (Renne et al., 1998); all errors are reported at the 2 standard deviation level of analytical precision. For each set of 10 laser-fusion analyses, we calculated both a range of apparent ages and a weighted mean age, where the weighting factors were the inverse of the variance for each fusion. For each incremental heating experiment, we calculated a weighted mean plateau age and an inverse isochron age. Age-elevation relationships were constructed using both datasets in order to evaluate rates and patterns of exhumation through the GHS.

4. Results

4.1. Age-elevation relationships

Individual cooling ages from both total fusion and step-heating analyses range from ~7 Ma at the base of the transect to ~21 Ma at the top. These results are summarized in Table 1; a more complete set of analytical results is found in the supplementary data in the Appendix [Tables A.1, A.2, and Figure A.3]. $^{40}Ar/^{39}Ar$ ages from all samples are shown as a

Table 1
Summary of $^{40}Ar/^{39}Ar$ cooling age data

			Single crystal laser-fusion experiment summary			Bulk step-heating experiment summary						
			Weighted age			Age spectra analysis				Isochron analysis		
Sample	Lithology	Elevation (m)	Age (Ma) ±2σ	MSWD	*N* of total	Age (Ma) ±2σ	^{39}Ar (k,%)	MSWD	*N* of total	Age (Ma) ±2σ	MSWD	40(*a*)/36(*a*) ±2σ
02WT48	Psammite	3280	7.88±0.13	60.0	10 of 10	7.05±0.16	82.8	7.36	15 of 24	6.94±0.28	7.44	313.2±37.8
02WT46	Schist	3501	8.69±0.18	79.9	10 of 10	8.16±0.11	67.7	3.44	12 of 18	8.39±0.26	2.94	258.7±39.6
02WT42	Schist	3672	8.71±0.44	104.0	10 of 10	8.82±0.11	69.6	2.42	12 of 16	8.88±0.20	2.55	286.8±25.6
02WT40	Migmatite	3780	8.79±0.49	110.1	10 of 10	Not analyzed: insufficient sample material				Not analyzed: insufficient sample material		
02WT38	Migmatite	3910	8.38±0.18	17.2	10 of 10	8.06±0.10	85.4	4.02	13 of 20	8.08±0.18	4.35	291.0±33.2
02WT36	Migmatite	4051	9.70±0.39	58.0	10 of 10	8.99±0.23	87.8	20.39	14 of 20	9.44±0.43	16.27	194.3±70.0
02WT35	Gneiss	4124	9.70±0.28	42.6	10 of 10	9.54±0.11	86.1	1.56	14 of 20	9.63±0.23	1.71	279.2±37.3
02WT34	Gneiss	4183	14.78±0.58	121.8	9 of 9	13.00±0.13	87.6	13.49	15 of 20	12.90±0.27	13.56	320.2±55.1
02WT33	Gneiss	4230	13.43±1.13	895.0	10 of 10	13.94±0.10	81.2	6.92	14 of 18	13.96±0.20	7.48	292.1±36.0
02WT32	Psammite	4280	20.66±0.79	280.1	10 of 10	20.91±0.23	90.7	1.06	14 of 18	20.81±0.32	1.09	306.4±26.4

n.b.: All ages reported relative to tcr-2a sanidine at 28.34 Ma; all errors reported as 2 s.d. of analytical precision.

function of elevation in Fig. 3. Our data show a prominent shift in the age-elevation relationship at ~4200 m, corresponding to a cooling age of ~10 Ma. A least-squares error weighted regression through the data from the lowermost six incremental heating results – between ~4120 m and 3280 m – yields a slope of 0.50 km/Myr with a correlation coefficient (*r*) of 0.75. There are not enough data to quantify the slope of the age-elevation relationship above 4120 m, but the three samples between 4120 and 4280 m clearly deviate from the lowermost samples, and delineate a much lower slope (≪0.1 km/Myr).

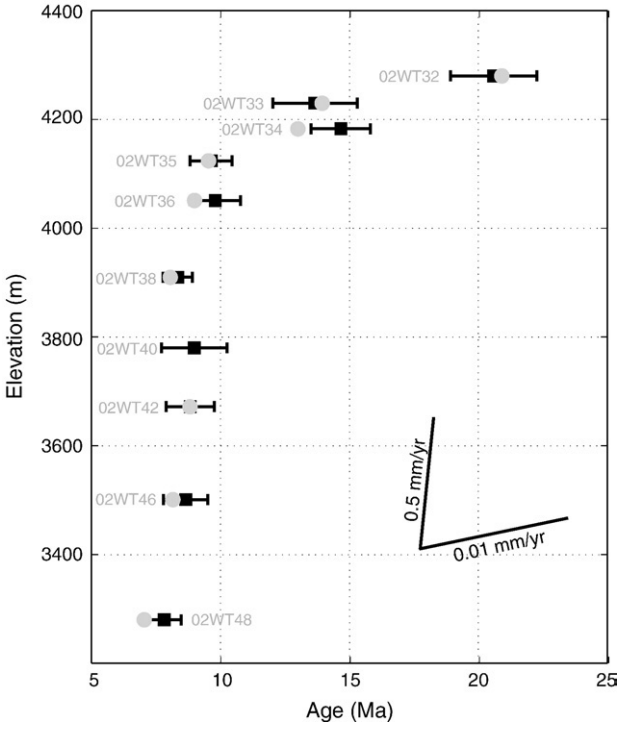

Fig. 3. Age-elevation relationships from biotite $^{40}Ar/^{39}Ar$ cooling age data. Black squares with error bars show the range of measured ages from ten replicate laser-fusion analyses. Grey dots show weighted plateau ages from incremental heating experiments (2σ analytical uncertainties for these analyses are smaller than dot sizes). Reference lines show slope of 0.5 mm/yr and 0.01 mm/yr exhumation rates. Sample names are adjacent to cooling age data.

As discussed below, the slope of an age-elevation relationship can be used as a proxy for the exhumation rate only if a stable closure isotherm depth is assumed (e.g., Reiners and Brandon, 2006). Thus the absolute slope of these relationships – both above and below the inflection at 10 Ma – should be interpreted with caution. Nonetheless, the prominent break in the slope of the age-elevation relationship at ~10 Ma clearly indicates a change in cooling rate, which requires a change in the overall kinematics of GHS exhumation at about that time.

4.2. Single-grain vs. bulk analyses

In nearly all cases, the range of cooling ages recorded from single-grain laser-fusion analyses overlaps with the weighted ages from incremental heating, suggesting that replicate single-grain laser-fusion analyses might be an efficient means of characterizing cooling ages from bedrock samples. However, the range of ages recorded by single-grain laser-fusion analyses is in all cases much larger than the calculated errors from incremental heating (Fig. 3), with the samples from the slowest-cooling (oldest) portion of the age-elevation transect generally exhibiting a wider range of apparent ages than those from the more rapidly cooling (youngest) portion of the transect. As shown below, this general result is consistent with what we would expect from a diverse population of grain sizes subject to slow cooling, and the spread in single-grain ages may in fact contain additional data that could be exploited in future studies to obtain more complete cooling histories from relatively small sample volumes.

For example, assuming that the range of cooling ages results entirely from differences in the effective closure temperature due to grain size variations, we can place our single-grain ages in context using the closure temperature equation of Dodson (1973):

$$T_c = \frac{E}{R \ln\left[\frac{ART_c^2 D_o}{a^2 E \mathrm{d}T/\mathrm{d}t}\right]} \quad (1)$$

where T_c is the effective closure temperature; E is the activation energy for volume diffusion, D_o is the diffusivity at infinite temperature; R is the gas constant; A is a geometric term (= 27 for a cylindrical diffusion geometry); a is the effective diffusion

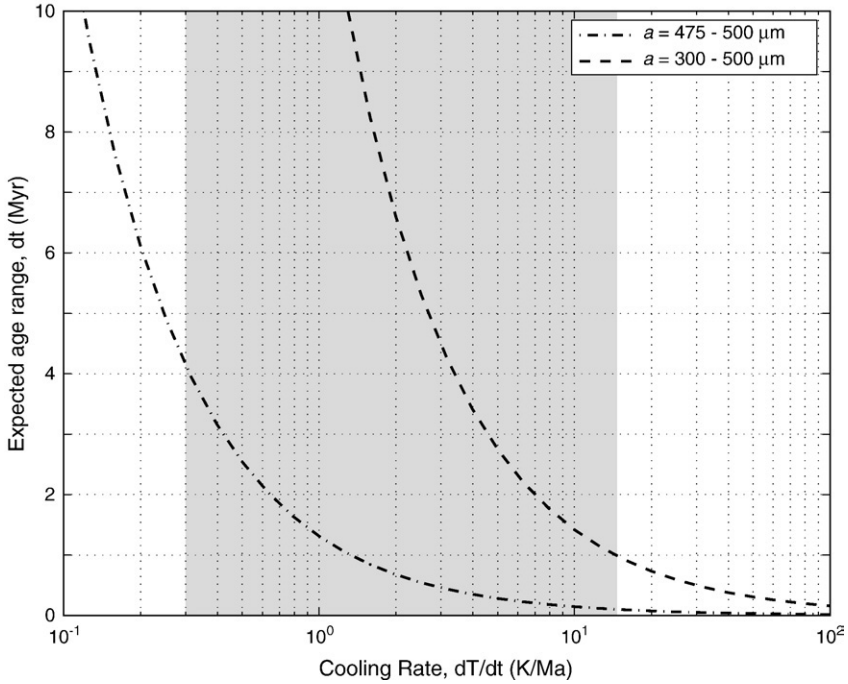

Fig. 4. Calculations based on Eqs. (1) and (2), showing predicted range of single-grain cooling ages as a function of cooling rate for Δa of 200 μm (dashed line); and 25 μm (dash-dot line). Grey box denotes the range of cooling rates estimated for our samples based on age-elevation relationships, under the simplifying assumption of a steady geothermal gradient of ~30 K/km. Note that the ranges of single-grain ages estimated from this study (<5 Myr) are well within the ranges predicted by closure temperature theory, even if only a narrow range of grain radii are present in each sample aliquot.

dimension; and dT/dt is the cooling rate. Noting that the range of cooling ages for a given sample is equivalent to the range of effective closure temperatures divided by the cooling rate, we can then calculate the expected age range from single-grain analyses as a function of cooling rate and the range of grain radii in the sample:

$$dt = \frac{dT_{c,a_{max}-a_{min}}}{dT/dt} \quad (2)$$

where $a_{max} - a_{min}$ is the range of grain radii contained within a given sample.

Solutions to Eqs. (1) and (2) are shown in Fig. 4. Since our single-grain aliquots were selected from a wide range of grain radii (250–500 μm) the range of single-grain ages we observe – less than 5 Myr and typically less than 2 Myr – is reasonable, and actually corroborates the slow cooling rates estimated from our age-elevation relationship. Because we did not initially design our study to exploit this range of single-grain cooling ages to constrain cooling rates, we did not measure individual grain radii prior to analyses. However, it is possible that future studies specifically designed to collect this information could construct more complete cooling histories from a relatively small number of single-grain total fusion analyses.

5. Discussion

5.1. Are the cooling ages meaningful?

In order to use our new dataset to make inferences about the influence of climate on regional tectonics, we must first ensure that our data can be reliably interpreted as reflecting the cooling of an intact tectonic block from metamorphic peak temperatures. The major complications that must be ruled out are: 1) post-closure deformation that might have juxtaposed two (or more) packages of rocks with different cooling histories; and 2) unresolved excess argon that renders the calculation of a cooling age from a $^{40}Ar/^{39}Ar$ ratio unreliable.

The first possibility can be largely discounted based on our field observations: the exposure along the north wall of the glaciated Langtang valley is exceptional, and we did not observe any indications in outcrop of substantial extensional deformation between the zones of apparent slow and moderate cooling rates. We can therefore presume that our entire age-elevation transect has remained as a tectonically intact block since its effective closure to diffusive argon loss.

While it is impossible to completely rule out the presence of unresolved excess argon in these samples – as is sometimes the case with Himalayan biotites (e.g., Godin et al., 2001; Viskupic et al., 2005) – there are at least four reasons to believe that excess argon is not responsible for the shift toward older cooling ages above ~4100 m. First, the isochron calculations reported here (Table 1, isochron for oldest sample shown in Fig. 5), consistently have $^{40}Ar/^{36}Ar$ intercepts within error of atmospheric composition, such that there is no direct indication in these samples of contamination by non-atmospheric initial $^{40}Ar/^{36}Ar$ (Kelley, 2002). Second, incremental heating experiments consistently yielded flat plateaus, without anomalously old or young steps in the early or late portions of the gas release (Roddick et al., 1980; Kelley, 2002). Third, there is not a direct correlation between the apparent ages of our samples and lithology: the kink

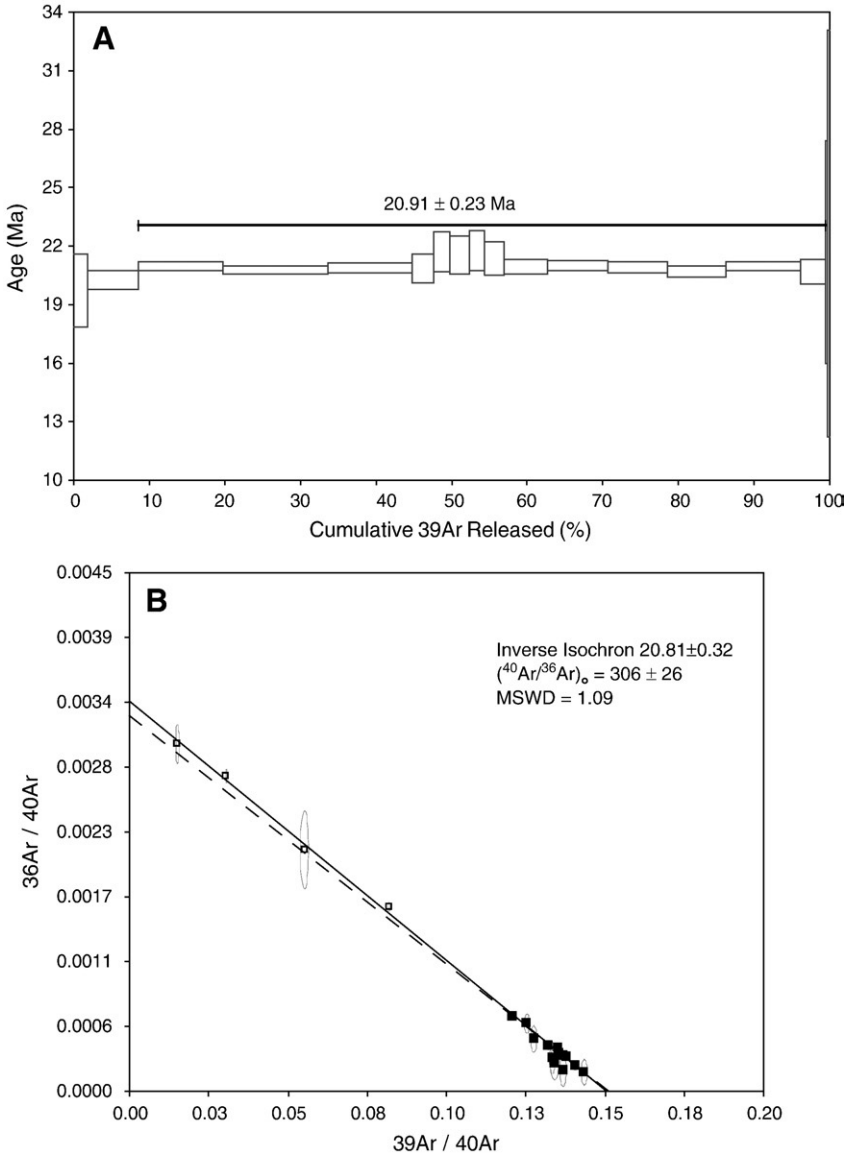

Fig. 5. Incremental heating plateau (A) and inverse isochron (B) results for sample 02WT32, collected from the top of the vertical transect. MSWD values from both calculations suggest no significant error over that predicted by analytical precision, and the $^{36}Ar/^{40}Ar$ intercept of the inverse isochron analysis is within error of atmospheric composition. Solid line in (B) is for isochron regression forced through atmospheric $^{36}Ar/^{40}Ar$ ratio; dashed line is regression with $^{36}Ar/^{40}Ar$ intercept as a free parameter. Open symbols in (B) are excluded from regression, i.e., the low and high temperature steps also not included in the plateau steps shown in (A).

in the age-elevation relationship occurs *within* a single lithology (Table 1), rather than at a lithologic contact (Baxter et al., 2002). And finally, the data are geologically reasonable: all of the cooling ages obtained from these samples are within the range of ages obtained from previous studies in the Langtang valley (Macfarlane, 1992), and the exhumation rate estimated from the lowermost six samples is consistent with the rate reported for a muscovite age-elevation transect in the nearby Marsyandi drainage over a similar time frame (Huntington et al., 2006). For all of these reasons, we can be confident that our data represent the cooling of these samples through the ~350 °C isotherm.

5.2. Change in kinematics at 10 Ma

The most striking feature of our age-elevation relationship is the prominent acceleration in the apparent exhumation rate at 10 Ma. This inflection can be added to a long list of other events that were occurring throughout the Himalaya at approximately the same time. For example, Molnar and others (e.g., Molnar et al., 1993; Molnar, 2005) note that 8±3 Ma witnessed the near-simultaneity of 1) the onset of basaltic volcanism and extension in Tibet; 2) the onset of folding in the Indo-Australian plate; 3) the initiation of river incision along the eastern margin of Tibet; and 4) the onset of folding in ranges bounding the northern Tibetan plateau. During this same timeframe, $\delta^{18}O$ and $\delta^{13}C$ records suggest changes in both rainfall and faunal assemblages in Asia; paleontological records indicate enhanced upwelling in the Arabian Sea which might correlate with enhanced Monsoonal circulation; and sedimentary records indicate changes in the quantity and caliber of material shed into both proximal basins and deep sea fan complexes (see Molnar (Molnar, 2005) and references therein). Our data suggesting an acceleration in

exhumation rate at ~10 Ma might corroborate the idea that the tectonic evolution of the Himalayan–Tibetan system was intimately linked to large-scale changes in Asian climate.

We also cannot rule out the possibility of a local tectonic driver for the observed change at ~10 Ma. For example, the growth of a "Lesser Himalayan Duplex" in the immediate footwall of the MCT (Robinson et al., 2003; Bollinger et al., 2006) would require a change to more vertical particle paths in the High Himalaya as material was accreted to this growing duplex. One set of numerical models describing such a phenomenon implicates a change in accretion velocity at ~8 Ma, which might be consistent with our data (e.g., Bollinger et al., 2006). As noted by Bollinger et al. (2006), however, these model predictions are also non-unique due to the wide range of unconstrained kinematic and thermal parameters, so that the ability of our dataset to corroborate such a model may be merely coincidental.

We note that the processes of ramp accretion and duplex growth as described by these tectonic models are also highly sensitive to the distribution of surface erosion. For example, analog and numerical models of accretionary orogens have shown that both the shape of the orogen and the locus of accretion are highly sensitive to the patterns of erosion (e.g., Davis et al., 1983; Whipple and Meade, 2004; Konstantinovskaia and Malavieille, 2005). Thus a "tectonic" driver such as the growth of a duplex or a change in accretion velocity must over the long term reflect a change in the patterns of surface erosion. Based on these considerations, our new dataset would therefore seem to corroborate the idea that deformation of the central Nepalese Himalaya is intimately tied to the distribution of surface erosion (Beaumont et al., 2001; Wobus et al., 2003).

5.3. Slow cooling before 10 Ma

An additional observation that is at least as interesting as the change in cooling rate at 10 Ma is the fact that our older data require very slow cooling rates between ~10 and 20 Ma. This result is perplexing given that the preponderance of published evidence would imply rapid exhumation of the High Himalaya at that time. For example, south-vergent thrusting on the Main Central Thrust appears to have begun by 23–20 Ma in at least some places along the Himalaya (e.g., Hodges, 2000), and this fault presumably accommodated much of the convergence between India and Eurasia at that time. Recent studies suggest that monsoon-like conditions were also in place by the Early Miocene (e.g., Guo et al., 2002; Sun and Wang, 2005), which would suggest that slip on the MCT should have been coupled to efficient surface erosion to exhume rocks from the Himalayan metamorphic core. Given these observations, why do our data suggest such slow cooling in central Nepal in the Early–Middle Miocene?

To answer this question, we must first consider the differences between cooling rates and exhumation rates in structurally complex and evolving orogenic systems. For example, the conversion of an age-elevation relationship into an exhumation rate requires a model for the thermal structure in the middle crust over the timeframe bracketed by the data; this thermal structure need not be temporally invariant. A complete model that describes the Miocene thermal evolution of the middle crust is both beyond the scope of this study and subject to unknowable free parameters. However, simple 1D thermal modeling studies indicate that abrupt increases in exhumation rates should be accompanied by a transient thermal state in which isotherms are advected upward along with the exhuming rock (e.g., Moore and England, 2001). For the argon system, the rate at which the closure isotherm is advected upward may be a large fraction of the total exhumation rate for millions of years following perturbation, such that the cooling rate preserved by an age-elevation relationship is not a good estimator of the exhumation rate at that time (e.g., Reiners and Brandon, 2006). Effectively there is a lag time between the onset of rapid exhumation and the onset of rapid cooling of mid-crustal rocks, during which time the slope of an age-elevation relationship substantially underestimates the exhumation rate.

In the context of our data, it is noteworthy that the initiation of the Main Central Thrust in Nepal is estimated to have occurred between 23 and 20 Ma (e.g., Hubbard and Harrison, 1989; Hodges et al., 1996), at the upper end of the cooling ages obtained in our transect. If slip on the MCT is taken to have begun at this time, then the argon closure isotherm is likely to have been advected upward along with the MCT hanging wall for the subsequent few million years, such that the slope of our age-elevation relationship might significantly underestimate the exhumation rate in the Early Miocene.

Perhaps more importantly, our data also say nothing of the exhumation *pathway* followed by this portion of the GHS through the closure interval. Most tectonic models of central Nepal include very low dips (<10°) on the northern and southern portions of the Main Himalayan Thrust, separated by a substantially steeper, crustal-scale ramp beneath the Himalayan front (e.g., Lyon-Caen and Molnar, 1983; Pandey et al., 1995; Avouac, 2003) (Fig. 1). This structural geometry requires that rocks currently exposed at the surface followed nearly horizontal exhumation pathways prior to reaching this ramp. Depending upon the degree to which isotherms were oblique to exhumation pathways during the closure interval, slow cooling therefore need not be synonymous with slow exhumation (e.g., Batt et al., 2000).

In this context, the change in cooling rate observed at ~10 Ma might actually be accounted for with little change in the overall evolution of the central Nepalese Himalaya. Instead, the observed inflection in our age-elevation relationship could simply reflect the point at which this particular package of rocks reached the base of the MHT ramp, at which time exhumation pathways became more vertical and less oblique to isotherms. Our dataset alone is insufficient to constrain the exact kinematics that would lead to this pattern, since the rocks that would allow us to estimate surface unroofing rates over this timeframe have been eroded and transported away from the Langtang valley. However, previous work in Himalayan foreland basins suggests very short lag times – and therefore rapid exhumation – in much of the Himalaya over the Early–Middle Miocene interval (White et al., 2002; Szulc et al., 2006). Such data suggest that rapid exhumation in the Early–Middle Miocene may have been synchronous with relatively slow cooling at deeper structural levels.

5.4. A way forward?

The problem that clearly emerges from the preceding discussion is that a wide range of scenarios can be envisioned to explain a dataset such as ours. Discriminating among such models relies on a suite of poorly constrained parameters, including: the spatial and temporal patterns of erosion from the Miocene to the present; the partitioning of tectonic convergence into overthrusting and underthrusting along the MHT and surface-breaking structures; the distribution of heat producing elements in the crust; the thermal diffusivity of the crust; the rate of accretion from the footwall to the hanging wall of the MHT; the rheology of the upper and lower crust; and the distribution of slip vectors in the middle and upper crust. This full suite of free parameters is probably impossible to constrain through the entire history of Himalayan growth.

On the other hand, any model that attempts to reconstruct a complete history of Himalayan exhumation *must* be true to the spatial and temporal patterns of cooling ages recorded in bedrock and nearby foreland basin sediments. Our interpretation is therefore that one clear way forward is to continue to obtain considerably better thermochronologic data throughout the Himalaya. Indeed, regional compilations for exhumation rates such as the one created by Sun and Wang (2005) for climate proxies are sorely needed if we hope to understand the orogen-scale links among precipitation, erosion, and tectonics. With substantially more data, we can then begin to separate regional trends from local perturbations, and to rule out models that cannot honor the data. The observation from our study that single-grain laser-fusion analyses from bedrock samples yield results that are consistent with incremental heating analyses suggests that any holes in such a regional compilation might be filled by new data relatively quickly and inexpensively. Such a regional compilation can then be used to reconstruct the spatial and temporal coherence of exhumation patterns in the Himalaya, which is a critical prerequisite to testing any model of climate-tectonic linkages in orogenic growth (e.g., Molnar, 2003; Hodges et al., 2004).

6. Conclusions

Our combined single-grain and bulk step-heating data from central Nepal indicate 1) very slow cooling of the Greater Himalayan Sequence in the Early Miocene; and 2) a substantial acceleration in cooling rate at ~10 Ma. If we make the simplifying assumption that the slopes of age-elevation relationships can be used as estimates of exhumation rates, these rates were ≪0.1 mm/yr prior to 10 Ma, and ~0.5 mm/yr between ~10 Ma and 7 Ma. At present, the lack of testable constraints on the thermal history of central Nepal through the Miocene requires that these absolute exhumation rates should be interpreted with caution. However, even acknowledging the potential complications to the thermal history, our interpretation that there was a substantial change in cooling rate at ~10 Ma – and therefore a change in kinematics – seems inescapable. Whether this change reflects transience in the thermal state of the Himalayan core, changes in exhumation pathway, or real changes to the system driven by exogenous variables such as climate, at this point must remain an open question. In any case, our study provides new data constraints on Himalayan exhumation that must be honored by any model describing the tectonic evolution of central Nepal.

Acknowledgements

This work was supported by NSF Tectonics grant EAR-008758 to KVH and KXW. Additional support was provided by a CIRES postdoctoral fellowship to CWW. We thank Ajay Sitaula and Himalayan Experience for logistical support, and Bill Olszewski for laboratory support. The manuscript benefited from the comments of two anonymous reviewers.

Appendix A. Supplementary data

Supplementary data associated with this article can be found, in the online version, at doi:10.1016/j.epsl.2008.02.019.

References

Avouac, J.P., 2003. Mountain building, erosion and the seismic cycle in the Nepal Himalaya. Adv. Geophys. 46. doi:10.1016/S0065-2687(1003)46001-46009.

Batt, G.E., Braun, J., Kohn, B.P., McDougall, I., 2000. Thermochronological analysis of the dynamics of the Southern Alps, New Zealand. GSA Bull. 112, 250–266.

Baxter, E.F., DePaolo, D.J., Renne, P.R., 2002. Spatially correlated anomalous $^{40}Ar/^{39}Ar$ "age" variations in biotites about a lithologic contact near Simplon Pass, Switzerland: a mechanistic explanation for excess Ar. Geochim. Cosmochim. Acta 66, 1067–1083.

Beaumont, C., Jamieson, R.A., Nguyen, M.H., Lee, B., 2001. Himalayan tectonics explained by extrusion of a low-viscosity crustal channel coupled to focused surface denudation. Nature 414, 738–742.

Bilham, R., Larson, K., Freymuller, J., 1997. GPS measurements of present-day convergence across the Nepal Himalaya. Nature 386, 61–64.

Bollinger, L., Henry, P., Avouac, J.P., 2006. Mountain building in the Nepal Himalaya: thermal and kinematic model. Earth Planet. Sci. Lett. 244, 58–71.

Bookhagen, B., Burbank, D.W., 2006. Topography, relief, and TRMM-derived rainfall variations along the Himalaya. Geophys. Res. Lett. 33. doi:10.1029/2006GL026037.

Burbank, D.W., Blythe, A.E., Putkonen, J., Pratt-Sitaula, B.A., Gabet, E.J., Oskin, M.E., Barros, A.P., Ojha, T., 2003. Decoupling of erosion and climate in the Himalaya. Nature 426, 652–655.

Clift, P.D., 2006. Controls on the erosion of Cenozoic Asia and the flux of clastic sediment to the ocean. Earth Planet. Sci. Lett. 241, 571–580.

Copeland, P., Harrison, T.M., Hodges, K.V., Maruejol, P., Le Fort, P., Pecher, A., 1991. An early Pliocene thermal disturbance of the Main Central Thrust, central Nepal; implications for Himalayan tectonics. J. Geophys. Res., B Solid Earth Planets 96, 8475–8500.

Davis, D., Suppe, J., Dahlen, F.A., 1983. Mechanics of fold-and-thrust belts and accretionary wedges. J. Geophys. Res. 88, 1153–1172.

Dodson, M.H., 1973. Closure temperature in cooling geochronological and petrological systems. Contrib. Mineral. Petrol. 40, 259–274.

Edwards, R.M., 1995. $^{40}Ar/^{39}Ar$ geochronology of the Main Central Thrust (MCT) region: evidence for Late Miocene to Pliocene disturbances along the MCT, Marsyangdi River valley, west-central Nepal Himalaya. J. Nepal Geol. Soc. 10, 41–46.

Garzione, C.N., Dettman, D.L., Quade, J., DeCelles, P.G., Butler, R.F., 2000. High times on the Tibetan Plateau: paleoelevation of the Thakkhola graben, Nepal. Geology 28, 339–342.

Godin, L., Parrish, R.R., Brown, R.L., Hodges, K.V., 2001. Crustal thickening leading to exhumation of the Himalayan metamorphic core of central Nepal:

insights from U–Pb geochronology and $^{40}Ar/^{39}Ar$ thermochronology. Tectonics 20, 729–747.
Grujic, D., Hollister, L.S., Parrish, R.R., 2002. Himalayan metamorphic sequence as an orogenic channel: insight from Bhutan. Earth Planet. Sci. Lett. 198, 177–191.
Guo, Z.T., Ruddiman, W.F., Hao, Q.Z., Wu, H.B., Qiao, Y.S., Zhu, R.X., Peng, S.Z., Wei, J.J., Yuan, B.Y., Liu, T.S., 2002. Onset of Asian desertification by 22 Myr ago inferred from loess deposits in China. Nature 416, 159–163.
Hodges, K.V., 2000. Tectonics of the Himalaya and southern Tibet from two perspectives. GSA Bull. 112, 324–350.
Hodges, K., 2003. Geochronology and thermochronology in orogenic systems. In: Rudnick, R.L. (Ed.), Treatise on Geochemistry, Volume 3: The Crust 3. Elsevier Science, Amsterdam, pp. 263–292.
Hodges, K., Wobus, C., Ruhl, K., Schildgen, T., Whipple, K., 2004. Quaternary deformation, river steepening and heavy precipitation at the front of the Higher Himalayan ranges. Earth Planet. Sci. Lett. 220, 379–389.
Hodges, K.V., Parrish, R.R., Searle, M.P., 1996. Tectonic evolution of the central Annapurna Range, Nepalese Himalayas. Tectonics 15, 1264–1291.
Hubbard, M.S., Harrison, T.M., 1989. $^{40}Ar/^{39}Ar$ age constraints on deformation and metamorphism in the Main Central thrust zone and Tibetan Slab, eastern Nepal Himalaya. Tectonics 8, 865–880.
Huntington, K.W., Blythe, A.E., Hodges, K.V., 2006. Climate change and Late Pliocene acceleration of erosion in the Himalaya. Earth Planet. Sci. Lett. 252, 107–118.
Inger, S., Harris, N., 1993. Geochemical constraints on leucogranite magmatism in the Langtang Valley, Nepal Himalaya. J. Petrol. 34, 345–368.
Kelley, S.A., 2002. Excess argon in K–Ar and Ar–Ar geochronology. Chem. Geol. 188, 1–22.
Konstantinovskaia, E., Malavieille, J., 2005. Erosion and exhumation in accretionary orogens: experimental and geological approaches. Geochem. Geophys. Geosyst. 6. doi:10.1029/2004GC000794.
Koppers, A.P., 2002. ArArCALC software for $^{40}Ar/^{39}Ar$ age calculations. Comput. Geosci. 28, 605–619.
Kroon, D., Steens, T., Troelstra, S.R., 1991. Onset of monsoonal related upwelling in the western Arabian Sea as revealed by planktonic foraminifers. Proc. Ocean Drill. Program Sci. Results 117, 257–263.
Lave, J., Avouac, J.P., 2001. Fluvial incision and tectonic uplift across the Himalayas of central Nepal. J. Geophys. Res. 106, 26561–26591.
Le Fort, P., 1975. Himalayas: the collided range. Present knowledge of the continental arc. Am. J. Sci. 275-A, 1–44.
Lyon-Caen, H., Molnar, P., 1983. Constraints on the structure of the Himalaya from an analysis of gravity anomalies and a flexural model of the lithosphere. J. Geophys. Res. 88, 8171–8191.
Macfarlane, A.M., The Tectonic Evolution of the Core of the Himalaya, Langtang National Park, Central Nepal, Ph.D., Massachusetts Institute of Technology, 1992.
Macfarlane, A.M., 1993. The chronology of tectonic events in the crystalline core of the Himalayas, Langtang National Park, central Nepal. Tectonics 12, 1004–1025.
Macfarlane, A., Hodges, K.V., Lux, D., 1992. A structural analysis of the Main Central thrust zone, Langtang National Park, central Nepal Himalaya. Geol. Soc. Amer. Bull. 104, 1389–1402.
Molnar, P., 2005. Mio-Pliocene growth of the Tibetan plateau and evolution of east Asian climate. Palaeontol. Electronica 8.
Molnar, P., 2003. Nature, nurture and landscape. Nature 426, 612–614.
Molnar, P., England, P., Martinod, J., 1993. Mantle dynamics, uplift of the Tibetan Plateau, and the Indian Monsoon. Rev. Geophys. 31, 357–396.
Moore, M.A., England, P.C., 2001. On the inference of denudation rates from cooling ages of minerals. Earth Planet. Sci. Lett. 185, 265–284.
Pandey, M.R., Tandukar, R.P., Avouac, J.P., Lave, J., Massot, J.P., 1995. Interseismic strain accumulation on the Himalayan crustal ramp (Nepal). Geophys. Res. Lett. 22, 751–754.
Pearson, O.N., DeCelles, P.G., 2005. Structural geology and regional tectonic significance of the Ramgarh thrust, Himalayan fold-thrust belt of Nepal. Tectonics 24. doi:10.1029/2003TC001617.
Reddy, S.P., Searle, M.P., Massey, J.A., 1993. Structural evolution of the High Himalayan gneiss sequence, Langtang Valley, Nepal. In: Treloar, P.J., Searle, M.P. (Eds.), Himalayan Tectonics Special Publication, vol. 74. The Geological Society, London, pp. 375–389.
Reiners, P.W., Brandon, M.T., 2006. Using thermochronology to understand orogenic erosion. Annu. Rev. Earth Planet. Sci. 34, 419–466.
Renne, P.R., Swisher, C.C., Deino, A.L., Karner, D.B., Owens, T.L., DePaolo, D.J., 1998. Intercalibration of standards, absolute ages and uncertainties in $^{40}Ar/^{39}Ar$ dating. Chem. Geol., Isot. Geosci. Sect. 145, 117–152.
Robinson, D.M., DeCelles, P.G., Garzione, C.N., Pearson, O.N., Harrison, T.M., Catlos, E.J., 2003. Kinematic model for the Main Central Thrust in Nepal. Geology 31, 359–362.
Roddick, J.C., Cliff, R.A., Rex, D.C., 1980. The evolution of excess argon in Alpine biotites — a $^{40}Ar/^{39}Ar$ analysis. Earth Planet. Sci. Lett. 48, 185–208.
Sorkhabi, R.B., Stump, E., Foland, K.A., Jain, A.K., 1996. Fission-track and $^{40}Ar/^{39}Ar$ evidence for episodic denudation of the Gangotri granites in the Garwhal Higher Himalaya, India. Tectonophysics 260, 187–199.
Sun, X., Wang, P., 2005. How old is the Asian monsoon system? Paleobotanical records from China. Palaeogeogr. Palaeoclimatol. Palaeoecol. 222, 181–222.
Szulc, A.G., Najman, Y., Sinclair, H.D., Pringle, M.S., Bickle, M., Chapman, H., Garzanti, E., Ando, S., Huyghe, P., Mugnier, J.L., Ojha, T.P., DeCelles, P.G., 2006. Tectonic evolution of the Himalaya constrained by detrital $^{40}Ar/^{39}Ar$, Sm–Nd and petrographic data from the Siwalik foreland basin succession, SW Nepal. Basin Res. 18, 375–391.
Thiede, R.C., Bookhagen, B., Arrowsmith, J.R., Sobel, E.R., Strecker, M.R., 2004. Climatic control on rapid exhumation along the southern Himalayan Front. Earth Planet. Sci. Lett. 222, 791–806.
Vannay, J.C., Hodges, K., 1996. Tectonometamorphic evolution of the Himalayan metamorphic core between Annapurna and Dhaulagiri, central Nepal. J. Metamorph. Geol. 14, 635–656.
Vannay, J.C., Grasemann, B., Rahn, M., Frank, W., Carter, A., Baudraz, V., Cosca, M., 2004. Miocene to Holocene exhumation of metamorphic crustal wedges in the NW Himalaya: evidence for tectonic extrusion coupled to fluvial erosion. Tectonics 23. doi:10.1029/2002TC001429.
Viskupic, K.M., Hodges, K.V., Bowring, S.A., 2005. Timescales of melt generation and the thermal evolution of the Himalayan metamorphic core, Everest region, eastern Nepal. Contrib. Mineral. Petrol. 149, 1–21.
Whipple, K.X., Meade, B.J., 2004. Controls on the strength of coupling among climate, tectonics and deformation in two-sided, frictional orogenic wedges at steady state. J. Geophys. Res. 109. doi:10.1029/2003JF000019.
White, N.M., Pringle, M., Garzanti, E., Bickle, M., Najman, Y., Chapman, H., Friend, P., 2002. Constraints on the exhumation and erosion of the High Himalayan Slab, NW India, from foreland basin deposits. Earth Planet. Sci. Lett. 195, 29–44.
Wobus, C.W., Hodges, K.V., Whipple, K.X., 2003. Has focused denudation sustained active thrusting at the Himalayan topographic front? Geology 31, 861–864.
Wobus, C., Heimsath, A., Whipple, K., Hodges, K., 2005. Active out-of-sequence thrust faulting in the central Nepalese Himalaya. Nature 434, 1008–1011.
Wobus, C.W., Whipple, K., Hodges, K.V., 2006. Neotectonics of the central Nepalese Himalaya: constraints from geomorphology, detrital $^{40}Ar/^{39}Ar$ thermochronology and thermal modeling. Tectonics 25. doi:10.1029/2005TC001935.